CIRCULAR-ELECTRIC MODE WAVEGUIDE COUPLERS AND JUNCTIONS FOR USE IN GYROTRON TRAVELING-WAVE AMPLIFIERS+

L. R. Barnett*, J. Mark Baird*, A. W. Fliflet*, V. L. Granatstein

Naval Research Laboratory

Washington, D.C.

Abstract

Recent gyrotron traveling-wave amplifier experiments in the TE_{01}° mode have led to the developing of 2-port and 4-port devices useful as input couplers, severs, and beam-rf separators for collector designs. We present analytical and experimental results.

Introduction

Recent experiments with a gyrotron traveling-wave amplifier operating in the TE_{01} circular waveguide mode [1] have spurred interest in developing circular-electric mode components. The recently reported amplifier experiments [1], which operate at 35 GHz, attained 30 dB gain in a single stage with 10 kW output. The useful small signal bandwidth was on the order of 1 GHz. The input coupler in this amplifier consisted of a TE_{01} coaxial mode to TE_{01} circular mode junction. The TE_{01} coaxial mode was produced from TE_{10} rectangular waveguide by a coaxial sector waveguide taper. A taper study is described in the companion paper [2]. The work has expanded beyond the original coupler development and has resulted in devices potentially useful in circular-electric mode amplifiers and oscillators or designs with circular-electric outputs [3,4].

Background

The initial design for the 2-port input coupler was derived from the Marcatili 4-port circular hybrid junction [5,6]. The 4-port hybrid is shown in Figure 1. An input at port A excites TE_{01}° and TE_{02}° propagating modes at z=0 in the gap region. The outer guide radius R_o is small enough to be cut off to circular-electric modes above TE_{02}° and therefore the excited TE_{03}° and above modes are evanescent. R_1 is placed at the TE_{02}° electric field null. When ℓ is adjusted such that

$$\left(\frac{2\pi}{\lambda_{g01}} - \frac{2\pi}{\lambda_{g02}}\right)\ell \cong (2n-1)\pi, \qquad (1)$$

where λ_{g01} and λ_{g02} are the waveguide wavelengths and n is an integer, then the TE_{01}° and TE_{02}° modes are in the phase relationship to couple most of the energy to port B in the $TE_{01}^{\circledcirc}$ mode. When:

$$\left(\frac{2\pi}{\lambda_{g01}} - \frac{2\pi}{\lambda_{g02}}\right)\ell \cong 2n\pi \qquad (2)$$

then most of the energy is coupled to port C in TE_{01}°.

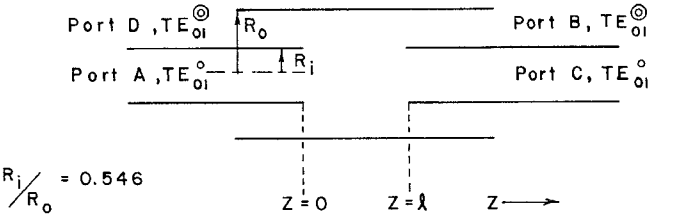

FIGURE 1. MARCATILI 4-PORT HYBRID COUPLER

Equations (1) and (2) do not take into account the small phase shifts introduced by evanescent fields. Power division can be accomplished by in-between adjustments of the gap length ℓ. This hybrid has good bandwidth (>20%) and a transmission loss at the center frequency of ~0.3 dB [5]. The device as is would make an effective sever for traveling-wave amplifiers. Marcatili made no further improvement [5] in the hybrid. We now show that the ratio of the wall radii R_i/R_o can be adjusted to obtain certain advantages. We extend the concepts to other uses and a more advanced coupling scheme using three modes.

The input coupler used in the 35 GHz gyrotron traveling-wave amplifier [1] was made by placing a plane reflector at $z = \ell/2$ to make a 2-port junction between port A in TE_{01}° and port D in TE_{01}. A sectorial waveguide taper from TE_{10} rectangular wave guide produced the TE_{01} coaxial input. A small hole in the reflector allowed entrance of the electron beam for interaction with the TE_{01}° mode in the central circular guide. The input coupler is shown in Figure 2 and it measured reflection properties in Figure 3. The experimental gyro-TWA [1] in which it was used is shown in Figure 4.

The devices thus far described utilize two propagating modes and will be referred to as 2-mode devices. Calculations and experiments show that 3-mode coupling is possible and such 3-mode devices have advantages over 2-mode devices in certain applications.

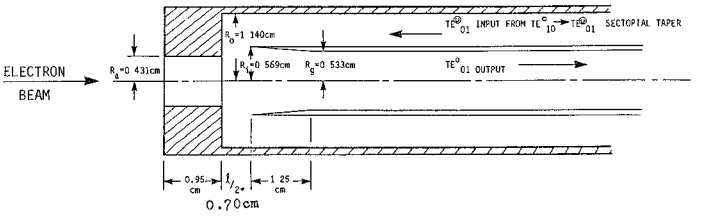

FIGURE 2. THE INPUT COUPLER, $TE_{10}^{\circledcirc}$ to TE_{01}°

+ Work supported by Naval Electronics System Command, Washington, D.C., Task #XF 54 581 007.

* B-K Dynamics, Inc., Rockville, Maryland.

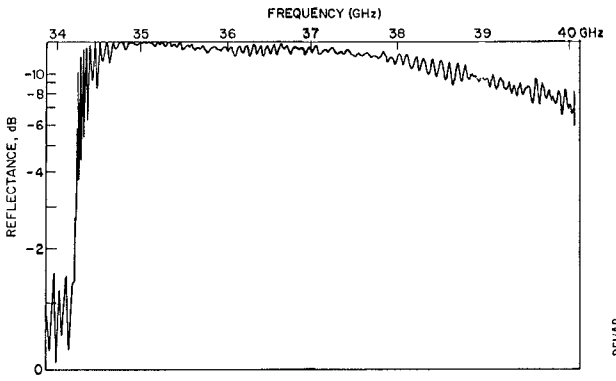

FIGURE 3. REFLECTION MEASUREMENT OF THE INPUT COUPLER OF FIGURE 2

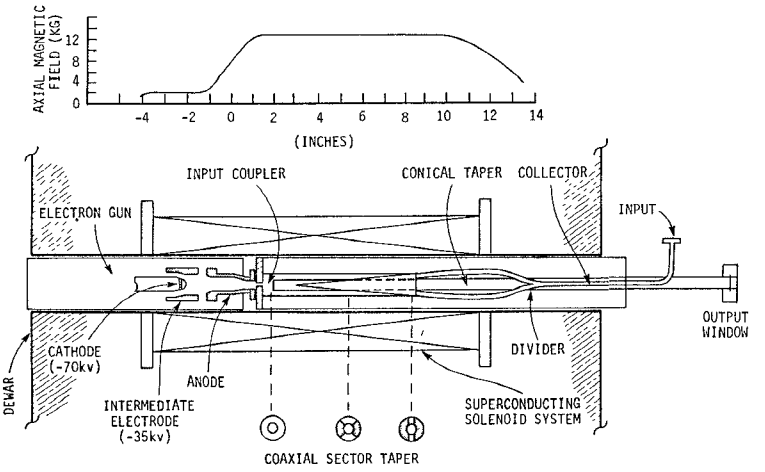

FIGURE 4. THE EXPERIMENTAL GYRO-TWA

Coupling Theory

The coupling coefficients can be found by solving for the mode voltages of the modes, given the boundary conditions and transverse electric field (or an approximate field) in the waveguide at the junction [7]. In this case:

$$\vec{E}_t = \sum_i \left(\vec{e}_i^{\,e} V_i^e + \vec{e}_i^{\,m} V_i^m \right) \tag{3}$$

where $\vec{E}_t$ is the transverse electric field at the junction (for instance, the TE°_{01} mode at z = 0 in Fig. 1), $\vec{e}_i^{\,e}$ are the TE mode vectors, $\vec{e}_i^{\,m}$ are the TM mode vectors, and V_i^e and V_i^m are TE and TM mode voltages respectively. By the orthogonality of the mode vectors then

$$\iint_S \vec{E}_t \cdot \vec{e}_i^{\,e}\, ds = V_i^e$$
$$\iint_S \vec{E}_t \cdot e_i^m\, ds = V_i^m \tag{4}$$

In this circular symmetrical geometry with TE_{on} excitation TM modes will not be excited. If the mode vectors are normalized

$$\iint_S \vec{e}_\ell^{\,e} \cdot \vec{e}_\ell^{\,e} = 1 \tag{5}$$

then

$$\iint_S \vec{e}_j^{\,e} \cdot \vec{e}_i^{\,e}\, ds = C_{ij}^e \tag{6}$$

defines the voltage coupling coefficient for excitation of $\vec{e}_i^{\,e}$ by $\vec{e}_j^{\,e}$.

The mode vectors are given by

$$\vec{e}^{\,e} = \hat{u}_z \times \nabla_t \psi^e \tag{7}$$

where for the circular electric modes

$$\psi^\circ_{on} \propto J_o\left(\frac{x'_{on}\rho}{R_o}\right) e^{-jk_{on}z}$$

$$\psi^\circ_{01} \propto \{ N'_o(k\rho R_i) J_o(k_\rho \rho) - J'_o(k_\rho R_i) N_o(k_\rho \rho) \} e^{-jk_{01}z} \tag{8}$$

As an example, using the above expressions, we find that the coupling coefficients to the TE°_{02} mode at z = 0 when excited by a TE°_{01} input at port A in Figure 1 is

$$C^{02} = \frac{2}{J_2(x'_{01})\, J_2(x'_{02}) R_i R_o} \int_o^{R_i} J_1\left(\frac{x'_{02}}{R_o}\rho\right) J_1\left(\frac{x'_{01}}{R_i}\rho\right) \rho\, d\rho$$

Figure 5 shows plots of the coupling coefficients to the first six TE°_{on} modes in the gap region as a function of R_i/R_o as excited by a TE°_{on} input at port A. Suppose the gap ℓ is adjusted for equation (2). Then coupling from port A to the output, port C, can readily be calculated. Calculating the coupling from a coaxial port to the modes and adjusting ℓ for equation (1) the coupling from port A to port B can be readily calculated. Figure 5 shows the power transmission from port A to port C for 2-mode coupling as a function of R_i/R_o. Three-mode coupling is accomplished by making the radius of the gap region above TE°_{03} cutoff. However, 3-mode coupling is successful only for specific values of R_o in order to obtain the proper relative phasing between the mode vectors as given by

$$\left(1 - \frac{f_{c02}^2}{f^2}\right)^{\frac{1}{2}} - \left(1 - \frac{f_{c03}^2}{f^2}\right)^{\frac{1}{2}} = m\left[\left(1 - \frac{f_{c01}^2}{f^2}\right)^{\frac{1}{2}} - \left(1 - \frac{f_{c02}^2}{f^2}\right)^{\frac{1}{2}}\right]$$

where f_{con} is the cutoff frequency of the TE°_{on} modes in the gap region and m is an integer. The 3-mode coupling shown in Figure 6 is for m = 2 and the smallest solution for R_o (still cutoff to TE°_{04}). Note that the 3-mode coupler transmission is more efficient than the 2-mode coupling, especially for $R_i/R_o < 0.6$. At $R_i/R_o = 0.69$ the coupling loss of both is the same, 0.07 dB. At this point the coupling to the TE°_{03} mode goes to zero. Not only is the 3-mode coupler generally more efficient, but is physically much larger than the 2-mode coupler. In the 35 GHz experimental couplers to be described, R_o = 1.181 cm for the 2-mode and R_o = 1.687 cm for the 3-mode solution given above. The gap length increased from 2.76 cm for the 2-mode to 6.71 cm for the 3-mode case. The increase in size

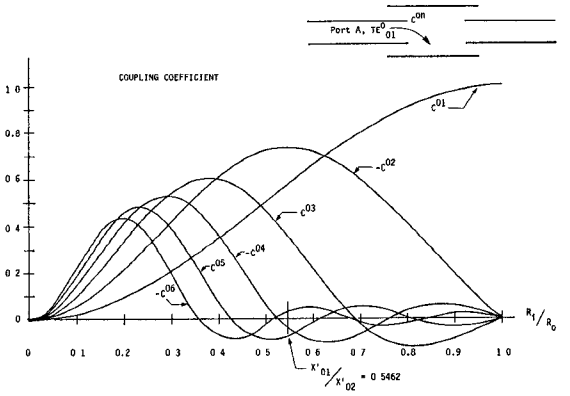

FIGURE 5. COUPLING COEFFICIENTS FROM PORT A

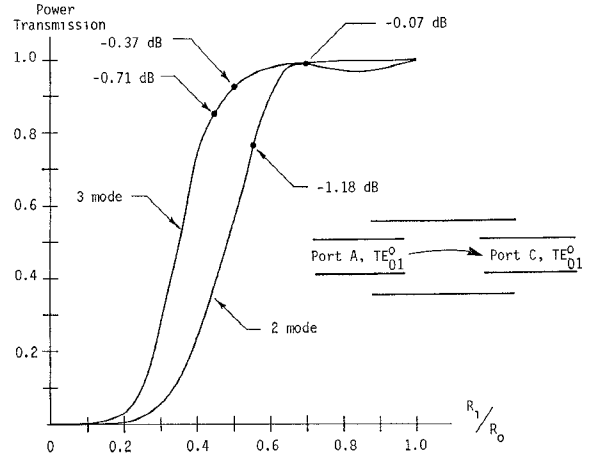

FIGURE 6. POWER TRANSMISSION FROM PORT A

is an advantage for using the outer wall as a beam collector or for a beam-rf separator which requires room for the beam to exit out of port B as guided by magnetic field lines. In this application we would also want R_i/R_o to be small and still maintain efficient coupling to port C. The 3-mode coupling is more efficient at the smaller ratios. Also, one could set $R_i/R_o = 0.69$ and utilize the TE^o_{04} mode as the third mode making the overall size even larger. Possibly even larger sizes could be made since coupling to the TE^o_{05} and higher modes is -26 dB or less and may not seriously impair performance.

We have performed experiments measuring the 2-mode and 3-mode coupling just described. In both couplers $R_i/R_o = x'_{01}/x'_{02} = 0.546$. The midband measured loss 35 to 36 GHz for the 2-mode coupler was 0.2 to 0.4 dB. The transmission bandwidth edges for 1 dB loss were ~34.0 to 40.0 GHz. The reflection coefficient from port A was ~-15 dB from 34.5 to 40.0 GHz and much lower at midband. Figure 7 shows the measured reflection coefficient of the 3-mode coupler. The 3-mode coupler has an almost rectangular window about 2 GHz wide centered at 35 GHz with a reflection coefficient of -23 dB or less at the band edges and going down to -30 dB or less at midband. The measured transmission loss was on the order of 0.05 dB over the 2 GHz band. The 2-mode coupler could be tuned to optimum performance at other center frequencies by varying the gap length ℓ. As expected, the 3-mode coupler could not be tuned and only worked well near its designed frequency of 35 GHz.

Some discrepancy is observed between calculations and experiments. The calculation of coupling for the 2-mode hybrid coupler of Figure 6 at $R_i/R_o = 0.546$ indicates about 1 dB loss should occur. Experiments by both Marcatili [5] and for this paper indicate a ~0.3 dB or less transmission loss occurs.

The coupling coefficients predicted in this paper were calculated on the basis that all the modes with significant coupling were below cutoff. The 2-mode coupling of Figure 6 was then calculated as if the TE_{03} and higher mode energy was being wasted, when in reality, the existence of coupling to evanescent modes results in modified coupling to the propagating modes and output power is coupled to all the ports instead of the desired one port. Figure 6 is then most accurate when coupling to evanescent modes is small, i.e., when $R_i/R_o \gtrsim .64$ in the 2-mode coupler and $R_i/R_o \gtrsim .48$ in the 3-mode coupling, etc. A fuller theory is in progress.

One interesting application for a beam-rf separator would be to start with large R_o (well above TE^o_{03} cutoff but below TE^o_{04} cutoff) at $z = 0$ for $R_i/R_o = 0.69$ and taper down to below TE^o_{03} cutoff at

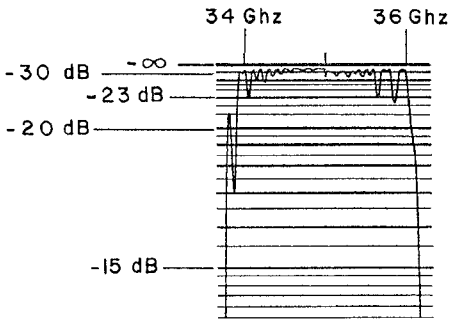

FIGURE 7. MEASURED REFLECTION COEFFICIENT FROM PORT A OF THE 3-MODE COUPLER OF FIGURE 5

$z = \ell$. The TE^o_{03} is not excited at $R_i/R_o = 0.69$ and hence no loss of match will occur. The electron beam could therefore travel almost straight through the device. Figure 8 shows a possible design (untested as yet) for operation at 35 GHz. The taper must not introduce significant mode conversion. Tuning could be accomplished with a sliding tube arrangement in the straight sections.

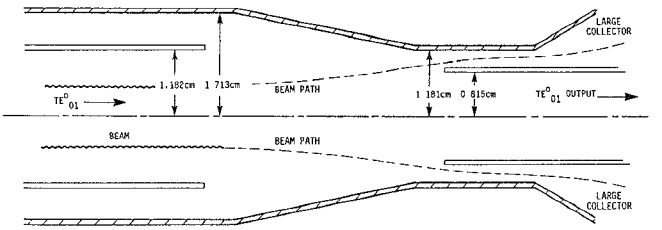

FIGURE 8. SUGGESTED BEAM-RF SEPARATOR

Conclusion

We conclude by noting that, by the analysis and experiments performed, wideband and efficient circular-electric mode coupling schemes can be used for several applications in circular-electric mode amplifiers and oscillators. In this summary we have only introduced a few possible applications and others become apparent as one investigates.

References

[1] L. R. Barnett, K. R. Chu, J. Mark Baird, V. L. Granatstein, A. T. Drobot, "Gain, Saturation, and Bandwidth Measurements of the NRL Gyrotron Travelling Wave Amplifier," International Electron Devices Meeting (IEDM) Technical Digest, pp 164-167, 1979.

[2] A. W. Fliflet, L. R. Barnett, J. Mark Baird, "Mode Coupling and Power Transfer in a Coaxial Sector Waveguide with a Sector Angle Taper," IEEE International Microwave Symposium, 1980.

[3] J. Mark Baird, "Survey of Fast Wave Tube Developments," IEDM Technical Digest, pp 156-163, 1979.

[4] M. E. Read, R. M. Gilgenback, A. J. Dudas, R. Lucey, K. R. Chu, V. L. Granatstein, "Operating Characteristics of a 35 GHz Gyromonotron," IEDM, pp 172-174, 1979.

[5] E. A. J. Marcatili, "A Circular-Electric Hybrid Junction and Some Channel-Dropping Filters," Bell System Technical Journal, pp 185-196, Jan. 1961.

[6] E. A. J. Marcatili, U.S. Patent 2,969,670; Nov. 1960.

[7] R. F. Harrington, Time Harmonic Electromagnetic Fields, Chapter 8, McGraw-Hill, 1961.